http://dx.doi.org/10.5012/bkcs.2013.34.12.3609

# Hydrothermal Synthesis of $LaCO_3OH$ and $Ln^{3+}$-doped $LaCO_3OH$ Powders under Ambient Pressure and Their Transformation to $La_2O_2CO_3$ and $La_2O_3$

**Min-Ho Lee and Woo-Sik Jung***

*School of Chemical Engineering, College of Engineering, Yeungnam University, Gyongsan 712-749, Korea*
**E-mail: wsjung@yu.ac.kr*
*Received August 27, 2013, Accepted September 9, 2013*

Orthorhombic and hexagonal lanthanum(III) hydroxycarbonate ($LaCO_3OH$) and $Ln^{3+}$-doped $LaCO_3OH$ ($LaCO_3OH:Ln^{3+}$, where Ln = Ce, Eu, Tb, and Ho) powders were prepared by a hydrothermal reaction under ambient pressure and characterized by thermogravimetry, powder X-ray diffraction, infrared and luminescence spectroscopy, and field-emission scanning electron microscopy. The polymorph of $LaCO_3OH$ depended on the reaction temperature, inorganic salt additive, species of $Ln^{3+}$ dopant, and solvent. The calcination of orthorhombic $LaCO_3OH:Ln^{3+}$ (2 mol %) powers at 600 ºC yielded a mixture of hexagonal and monoclinic $La_2O_2CO_3:Ln^{3+}$ powders. The relative quantity of the latter increased with decreasing ionic radius of the $Ln^{3+}$ dopant ion and increasing doping concentrations. On the other hand, the calcination of hexagonal $LaCO_3OH:Ln^{3+}$ (2 mol %) powders at 600 ºC resulted in a pure hexagonal $La_2O_2CO_3:Ln^{3+}$ powder, regardless of the species of $Ln^{3+}$ ions (Ln = Ce, Eu, and Tb). The luminescence spectra of $LaCO_3OH:Ln^{3+}$ and $La_2O_2CO_3:Ln^{3+}$ were measured to examine the effect of their polymorph on the spectra.

**Key Words :** Hydrothermal reaction, $LaCO_3OH$, $La_2O_2CO_3$, Polymorph, Luminescence

## Introduction

Trivalent lanthanide ($Ln^{3+}$) ions have high affinity to the carbonate ($CO_3^{2-}$) ion, as evidenced by the occurrence of stable minerals such as $(La,Ce,Nd)_2(CO_3)_3{\cdot}8H_2O$ (lanthanite), $(La,Ce)_2(CO_3)_3{\cdot}4H_2O$ (calkinsite), and $(La,Ce)(F,OH)CO_3$ (bastnaesite).[1] Of the lanthanum carbonates, $LaFCO_3$ and $LaCO_3OH$ are useful starting materials for their thermal decomposition products such as LaOF, $La_2O_2CO_3$, and $La_2O_3$, which are attractive host materials of phosphors.[2-6] $LaFCO_3$ powders exist as a single polymorph (hexagonal one), whereas $LaCO_3OH$ powders exist in two polymorphs, *i.e.*, orthorhombic (*o*-) and hexagonal (*h*-) $LaCO_3OH$. To date, $LaCO_3OH$ powders have been synthesized using a variety of methods, including the hydrolysis of $LaCl_3$-trichloroactic acid solution by ammonia,[7] hydrolysis of La(III) carbonate under high[8] and ambient[9] pressure, reaction of LaBrOH with $CO_2$,[9] solvothermal reaction of $La_2O_3$ in a mixed solvent of ionic liquid and water,[10] and solvent-free dissociation of La(III) acetate hydrate under autogenic pressure at 700 ºC.[11] $LaCO_3OH$ powders have been also prepared by a hydrothermal reaction in an autoclave using the following reagents: $LaCl_3$ and thiourea,[12,13] $La(NO_3)_3$ and urea,[4,14] $La(NO_3)_3$, glucose, and acrylamide,[15] $La_2O_3$ and glycine,[16] $LaCl_3$ and gelatin,[17] La(oleate)$_3$ and aqueous *tert*-butylamine,[18] $La^{3+}$-EDTA complex and urea,[19] and $La(NO_3)_3$ and $NH_4HCO_3$.[20] According to these reports, most $LaCO_3OH$ powders prepared by a hydrothermal reaction in an autoclave had the hexagonal polymorph. On the other hand, *o*-$LaCO_3OH$ powders sometimes formed in an autoclave.[15,17] $LaCO_3OH$ powders can also be prepared by a hydrothermal reaction without the need for an autoclave,[3,21] as for $LaFCO_3$ powders.[22] To date, there are still no reports on the factors determining the polymorph of $LaCO_3OH$ powders obtained by a hydrothermal reaction under ambient pressure.

In this study, $LaCO_3OH$ powders were prepared by a hydrothermal reaction from the solution containing $La(NO_3)_3$ and urea without the need for an autoclave. The effects of the reaction temperature, inorganic salt additive, species of $Ln^{3+}$ dopant, and solvent on the polymorph of $LaCO_3OH$ powders were investigated. Urea is used widely as the precipitation reagent of metal ions because it thermally decomposes into $NH_3$ and $CO_3^{2-}$ ions in neutral and basic aqueous solutions.[23] The as-prepared $LaCO_3OH$ powders were characterized by powder X-ray diffraction (XRD), Fourier transformation infrared (IR) spectroscopy, thermogravimetric (TG) and differential thermal analysis (DTA), and field-emission scanning electron microscopy (FE-SEM). $Ln^{3+}$-doped $LaCO_3OH$ ($LaCO_3OH:Ln^{3+}$, where Ln = Ce, Eu, Tb, and Ho) powders were also synthesized to determine the effect of dopants on the polymorph of $La_2O_2CO_3$ and $La_2O_3$. The luminescence spectra of the $LaCO_3OH:Eu^{3+}$ and $La_2O_2CO_3:Eu^{3+}$ powders were measured to examine the effect of their polymorph on the spectra.

## Experimental Section

**Synthesis of $LaCO_3OH$ and $LaCO_3OH:Ln^{3+}$ Powders.** All starting materials, $La(NO_3)_3{\cdot}6H_2O$ (99.9%), $Ce(NO_3)_3{\cdot}6H_2O$ (99.99%), $Eu(NO_3)_3{\cdot}6H_2O$ (99.9%), $Tb(NO_3)_3{\cdot}6H_2O$ (99.99%), $Ho(NO_3)_3{\cdot}5H_2O$ (99.9%), and urea (99.0%) were purchased from Sigma-Aldrich Co. and used as-received without further purification. In a typical synthesis of $LaCO_3OH$ powder, 8.66 g ($2.00 \times 10^{-2}$ mol) of $La(NO_3)_3{\cdot}6H_2O$ and 6.01 g (1.00

$\times 10^{-1}$ mol) of urea were dissolved in 50 mL of a mixed solvent of ethylene glycol (EG) and water. EG to water volume ratios were 9:1, 8:2, 7:3, 6:4, 5:5, 2:8, and 0:10. The solution was boiled for 24 h under ambient pressure and cooled to room temperature. Sequentially, the white precipitate was separated by centrifugation, washed several times with water and ethyl alcohol, and dried in an oven at 70 °C. The quantities of $La(NO_3)_3 \cdot 6H_2O$, urea, and solvent were kept constant through this study. $LaCO_3OH:Ln^{3+}$ powders were prepared in the same way as that for $LaCO_3OH$ powders except that $Ln(NO_3)_3$ salts (2 mol %) were added to the solution containing 8.49 g of $La(NO_3)_3 \cdot 6H_2O$.

**Characterization.** The $LaCO_3OH$ powders and their thermal decomposition products were characterized by powder XRD (PANalytical X'Pert PRO MPD X-ray diffractometer) using Cu-Kα radiation operating at 40 kV and 30 mA and IR spectroscopy (Nicolet 6700, Thermo Scientific). The TG and DTA curves of $LaCO_3OH$ powders were recorded on an SDT Q600 apparatus (TA Instruments) at a heating rate of 10 °C/min. The morphology of the product powders was investigated by FE-SEM (Hitachi S-4200). The luminescence spectra of $LaCO_3OH:Eu^{3+}$ and $La_2O_2CO_3:Eu^{3+}$ were measured at ambient temperature on a JASCO FP-6500 spectrofluorometer with a 150 W xenon lamp.

## Results and Discussion

**Synthesis of $LaCO_3OH$ and $LaCO_3OH:Ln^{3+}$ Powders.** The $LaCO_3OH$ powders were synthesized by a hydrothermal reaction in various mixed solvents such as water-EG and water-DMSO, without the use of an autoclave. EG is used widely as a solvent to control the morphology of many materials.[4,5,24,25] EG is mixed with water at any ratio. The boiling point (B.P.) of the water-EG solution can be controlled easily by EG to water volume ratio. Recently, Mao *et al.* prepared $LaCO_3OH$ powders by a hydrothermal reaction in water-EG solvents using an autoclave and reported that the volume ratio had remarkable effect on the species and morphology of the particles.[4] Boiling (B. P. ≥ 118 °C) in the mixed solvents containing more than 70 volume % EG gave a pure *h*-$LaCO_3OH$ powders (Figure 1(a)). In contrast, *o*-$LaCO_3OH$ powders mixed with a very small amount of *h*-$LaCO_3OH$ powders were obtained by boiling (B. P. ≤ 110 °C) in mixed solvents containing less than 60 volume % EG (Figure 1(b)). These results are considerably different from those obtained by hydrothermal synthesis in an autoclave,[4] where *h*-$LaCO_3OH$ powders were obtained in mixed solvents containing less than 50 volume % EG, whereas $La_2(CO_3)_3(H_2O)_8$ and $La_2(CO_3)_3(OH)_2$ were obtained in mixed solvents containing more than 50 volume % EG.

To determine if the reaction temperature is a major factor influencing the polymorph of the $LaCO_3OH$ powders, the $LaCO_3OH$ powders were prepared in mixed solvents of water and DMSO (B. P. = 189 °C). Boiling (B. P. = 125 °C) the solution in a mixed solvent containing 80 volume % DMSO yielded a pure *o*-$LaCO_3OH$ phase, whereas boiling

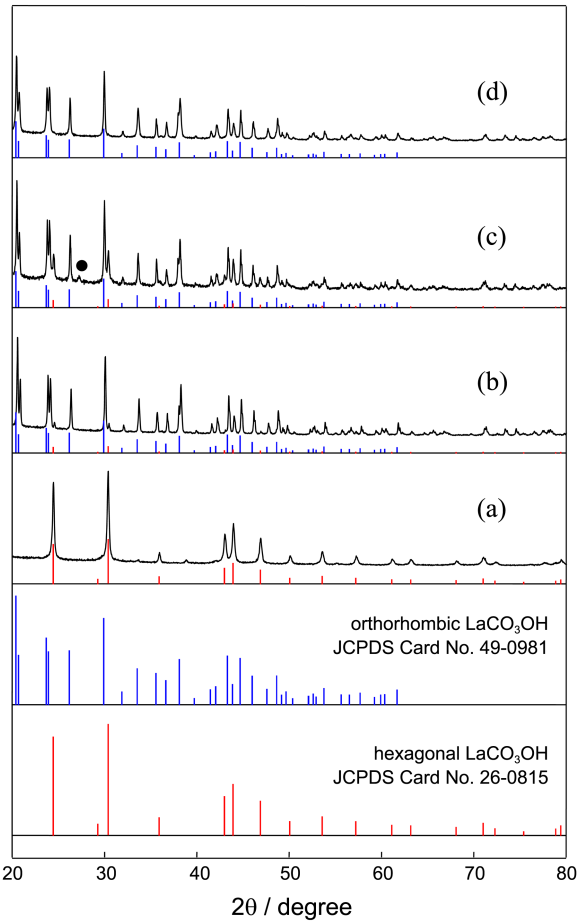


**Figure 1.** XRD patterns of samples obtained by a hydrothermal reaction in water-EG solvents with (a) ≥ 70 and (b) ≤ 60 volume % of EG, (c) in water-DMSO containing 90 volume % DMSO, and (d) in water added with $KNO_3$: ●, unidentified phase.

(B. P. = 143 °C) the solution in a mixed solvent containing 90 volume % DMSO yielded an *o*-$LaCO_3OH$ powder mixed with a small amount of *h*-$LaCO_3OH$ powder, as shown in Figure 1(c). Therefore, even boiling at a higher B. P. in the water-DMSO system than in the water-EG system did not yield pure *h*-$LaCO_3OH$ powders. This suggests that the polymorph of $LaCO_3OH$ powders is determined not only by the reaction temperature but also by the solvent. Further evidence of the reaction temperature being not the main factor determining the polymorph of the $LaCO_3OH$ powders was provided by the formation of *o*-$LaCO_3OH$ powders in an autoclave at very high reaction temperatures.[15,17] The reason why the phase of the $LaCO_3OH$ powders depends on the solvent remains unclear. EG appears to be a favorable solvent for the preparation of *h*-$LaCO_3OH$ powders at relatively low temperatures. In contrast to DMSO, EG has similar characteristics to water in that EG molecules can form hydrogen-bonded networks. These characteristics of EG may induce variations in the morphology and polymorph by changing the volume ratio of water-EG solvents.

Low reaction temperatures in hydrothermal reactions in which $La(NO_3)_3 \cdot 6H_2O$ and urea were used as reagents resulted in the formation of pure *o*-$LaCO_3OH$ powders,[3] but

caused a low yield. For example, the reaction temperature of 66 °C in water caused the formation of *o*-$LaCO_3OH$ powders in 24% yield. This yield increased with increasing reaction temperatures, but increasing the temperatures caused the formation of *h*-$LaCO_3OH$ powders. Therefore, it is difficult to synthesize pure *o*-$LaCO_3OH$ powders in high yield using $La(NO_3)_3{\cdot}6H_2O$ as the $La^{3+}$ ion source. Pure *o*-$LaCO_3OH$ powders were obtained in *ca.* 100% yield by boiling aqueous solution containing $La(NO_3)_3{\cdot}6H_2O$, urea, and $KNO_3$, in which the $KNO_3$ to $La(NO_3)_3{\cdot}6H_2O$ mole ratio was two and higher (Figure 1(d)). The addition of 0.100 mol $NaNO_3$ or $NH_4NO_3$, however, yielded a mixture of *o*- and *h*-$LaCO_3OH$ powders with almost equal quantity. Inorganic ions have been used to control the morphology of nanomaterials.[26,27] The effect of salts on the phase has also been reported in the synthesis of nanostructured orthorhombic and hexagonal $EuF_3$ from a reaction of $Eu(NO_3)_3{\cdot}6H_2O$ with XF ($X = H^+$, $NH_4^+$, and alkali ions).[27]

In a mixed solvent containing 80 volume % EG, doping $LaCO_3OH$ with 2 mol % $Ln^{3+}$ (Ln = Ce and Eu) into $LaCO_3OH$ yielded *h*-$LaCO_3OH$:$Ln^{3+}$, but the doping with 2 mol % $Tb^{3+}$ and $Ho^{3+}$ ions yielded *h*-$LaCO_3OH$:$Tb^{3+}$ mixed with a very small amount of *o*-$LaCO_3OH$:$Tb^{3+}$ and *o*-$LaCO_3OH$:$Ho^{3+}$ mixed with a smaller amount of *h*-$LaCO_3OH$:$Ho^{3+}$, respectively. This suggests that doping with $Ln^{3+}$ ion having smaller ionic radius is more effective in inducing the formation of *o*-$LaCO_3OH$. This doping effect on the polymorph can be explained in terms of the phase diagrams for $La_2O_3$-$H_2O$-$CO_2$ ternary systems for the lanthanide series, which were established by Kutty *et al*.[28] Based on the phase diagrams, they showed that the stable polymorph of $LaCO_3OH$ is orthorhombic for elements with atomic number 64 and higher. On the other hand, doping $LaCO_3OH$ with 2 mol % $Ln^{3+}$ ions in aqueous solution containing $KNO_3$ resulted in pure *o*-$LaCO_3OH$:$Ln^{3+}$, regardless of the presence of $Ln^{3+}$ ions.

**Characterization of $LaCO_3OH$ Powders.** The *h*- and *o*-$LaCO_3OH$ powders, which were obtained in a mixed solvent containing 80 volume % EG and aqueous solution containing $KNO_3$, respectively, were characterized by TG, IR spectroscopy, and SEM. Figure 2 shows the TG and DTA curves of the $LaCO_3OH$ powders. The TG curves indicated the following decomposition processes:

$$LaCO_3OH{\cdot}xH_2O \rightarrow LaCO_3OH \quad (1)$$

$$2\ LaCO_3OH \rightarrow La_2O_2CO_3 + H_2O + CO_2 \quad (2)$$

$$La_2O_2CO_3 \rightarrow La_2O_3 + CO_2 \quad (3)$$

The observed weight losses accompanied by the decomposition of *h*- and *o*-$LaCO_3OH{\cdot}xH_2O$ to $La_2O_3$ were 28.9 and 26.1%. Therefore, the values of x for *h*- and *o*-$LaCO_3OH{\cdot}xH_2O$ were estimated to be 0.73 and 0.25, respectively. The first weight loss in the temperature range from room temperature to *ca.* 400 °C was assigned to the loss of adsorbed water ($xH_2O$), as expressed in equation (1). The abrupt weight losses above *ca.* 400 °C and 700 °C were attributed to reactions (2) and (3), respectively. The theoretical weight loss accompanied by reactions (2) and (3) is 15.0% and 11.9%, which were similar to 14.6% and 11.3% observed for *o*-$LaCO_3OH$, respectively. A comparison of slopes in the temperature range from 500 to 700 °C indicated that the rate of the $LaCO_3OH$ to $La_2O_2CO_3$ transformation is much slower for *h*- than *o*-$LaCO_3OH$. DTA curves showed that reactions (2) and (3) were endothermic. In addition, the endothermic peak for reaction (2) appeared at higher

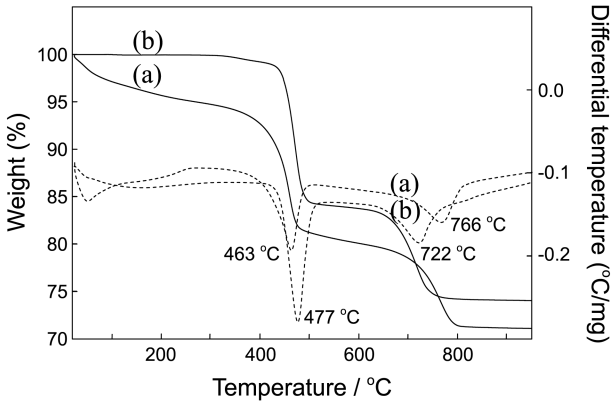


**Figure 2.** TG (solid line) and DTA (dotted line) curves of (a) *h*- and (b) *o*-$LaCO_3OH$ powders.

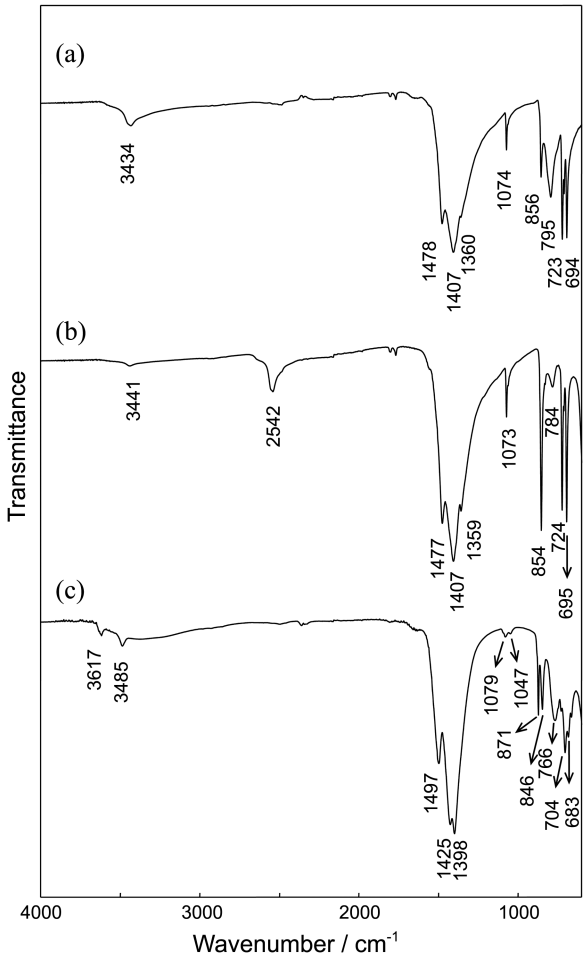


**Figure 3.** IR spectra of (a) *o*-$LaCO_3OH$, (b) *o*-$LaCO_3OD$, and (c) *h*-$LaCO_3OH$ powders.

temperature for *o*-$LaCO_3OH$ than for *h*-$LaCO_3OH$, whereas the opposite was observed for reaction (3).

Figure 3 shows IR spectra of the *h*- and *o*-$LaCO_3OH$ powders. The IR spectrum (Figure 3(a)) of the *o*-$LaCO_3OH$ powder was similar to those of *o*-$LaCO_3OH$ powders obtained by boiling aqueous solution containing $La(NO_3)_3$ and urea[3] and by a reaction of LaBrOH with $CO_2$[9] but different from that of an *o*-$LaCO_3OH$ powder prepared in an autoclave.[17] The OH-stretching band appeared at 3443 $cm^{-1}$ for *o*-$LaCO_3OH$ and at 3617 and 3484 $cm^{-1}$ for *h*-$LaCO_3OH$. In many reports, the two bands for *h*-$LaCO_3OH$ were assigned to structural OH and adsorbed $H_2O$,[11,14,16,18] but they can both be assigned to the stretching bands of two nonequivalent structural OH groups.[9] The very broad band centered at *ca*. 3300 $cm^{-1}$ in Figure 3(c) was ascribed to the OH-stretching of adsorbed $H_2O$ because the IR spectrum measured after drying at 200 °C for 2 days showed that the stretching bands of two structural OH groups were invariant and the very broad band centered at *ca*. 3300 $cm^{-1}$ almost disappeared. The bands below 1500 $cm^{-1}$ in Figure 3 were assigned to the vibrational modes of coordinated $CO_3^{2-}$ ion. Four normal modes of free $CO_3^{2-}$ ion appear at 1063 $cm^{-1}$ ($\nu_1$), 879 $cm^{-1}$ ($\nu_2$), 1415 $cm^{-1}$ ($\nu_3$), and 680 $cm^{-1}$ ($\nu_4$).[29] Lowering of symmetry from $D_{3h}$ to $C_{2v}$ or $C_s$ by coordination causes the presence of an IR-inactive $\nu_1$ mode and splitting of the degenerate $\nu_3$ and $\nu_4$ modes.[30] As shown in Figure 3(a), $\nu_3$ and $\nu_4$ modes were split into two peaks (1478 and 1407 $cm^{-1}$, 723 and 694 $cm^{-1}$, respectively) and $\nu_1$ mode was observed at 1074 $cm^{-1}$ for *o*-$LaCO_3OH$. The peak at 856 $cm^{-1}$ was attributed to the $\nu_2$ mode. The peak at 795 $cm^{-1}$ was assigned to the deformation vibration of $CO_3^{2-}$ ion rather than some vibration of structural OH.[11] This assignment is based on a comparison in the IR spectra (Figures 3(a) and 3(b)) between the *o*-$LaCO_3OH$ and *o*-$LaCO_3OD$ powders. The latter powder was prepared using $D_2O$ (99.9 atom% D, Sigma-Aldrich) instead of $H_2O$ as a solvent. The structural OD-stretching band appeared at 2542 $cm^{-1}$ in Figure 3(b). Assuming that the force constant is the same in structural OH and OD groups, the structural OD-stretching frequency was estimated to be 2512 $cm^{-1}$, which is close to that observed. Except the structural OD-stretching band, each peak in Figure 3(b) appeared at almost the same position as the corresponding peak in Figure 3(a), showing that the peak at 795 $cm^{-1}$ is associated with deformation vibration of $CO_3^{2-}$ ion. The IR spectrum (Figure 3(c)) of the *h*-$LaCO_3OH$ powder was more complicated due to multiple splitting of all the modes. The multiple splitting can be interpreted in terms of nonequivalent carbonate groups.[30]

The morphology of the *h*- and *o*-$LaCO_3OH$ powders was observed by SEM. As shown in Figure 4, the *h*-$LaCO_3OH$ particles were almost spherical with mean particle size of ~600 nm, whereas the *o*-$LaCO_3OH$ particles were rhombic.[3]

**Transformation of $LaCO_3OH:Ln^{3+}$ to $La_2O_2CO_3:Ln^{3+}$ and $La_2O_3:Ln^{3+}$.** As shown in Figure 2, $LaCO_3OH$ decomposed to $La_2O_3$ through $La_2O_2CO_3$. Figure 5 shows XRD patterns of the powders obtained by calcination of *h*- and *o*-$LaCO_3OH$ powders at 600 and 800 °C for 2 h. The calcination of both powders at 600 °C gave the hexagonal (*h*-) $La_2O_2CO_3$ (JCPDS Card No. 37-0804), as in other studies.[4,15] As shown in Figures 5(a) and 5(b), the *h*-$La_2O_2CO_3$ powder derived from *o*-$LaCO_3OH$ exhibited narrower diffraction peaks than that from *h*-$LaCO_3OH$, due to the larger particle size. The XRD pattern (Figure 5(c)) of the powder obtained by calcination of *o*-$LaCO_3OH$ at 800 °C was indexed to hexagonal (*h*-) $La_2O_3$ (JCPDS Card No. 05-0602), as for that of the powder obtained by calcination of *h*-$LaCO_3OH$ at 800 °C.

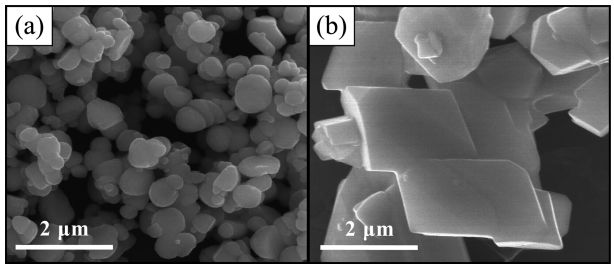


**Figure 4.** SEM images of (a) *h*- and (b) *o*-$LaCO_3OH$ powders.

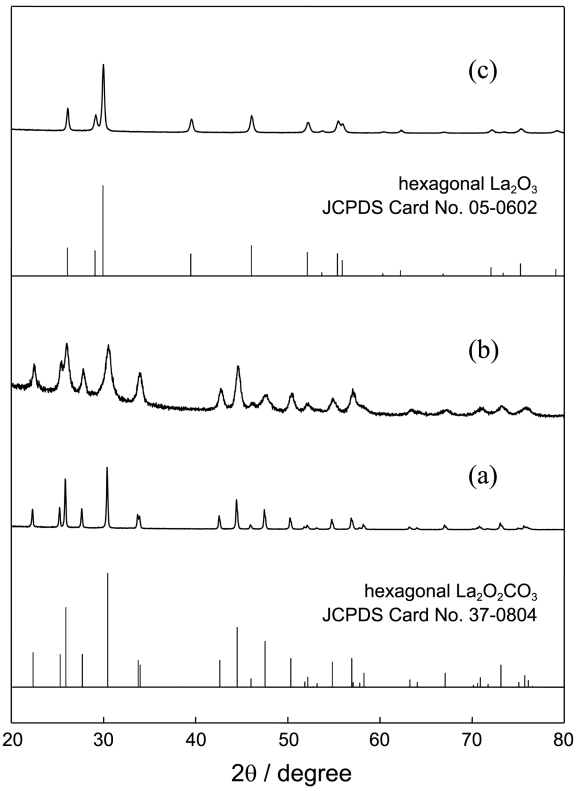


**Figure 5.** XRD patterns of samples obtained by calcination of (a) *o*- and (b) *h*-$LaCO_3OH$ at 600 °C for 2 h and (c) by calcination of *o*-$LaCO_3OH$ at 800 °C for 2 h.

The effect of dopants on the polymorph of $La_2O_2CO_3$ and $La_2O_3$ was examined with various dopants and concentrations. The calcination of *h*-$LaCO_3OH:Ln^{3+}$ (2 mol %, Ln = Ce, Eu, and Tb) at 600 °C for 2 h yielded *h*-$La_2O_2CO_3$ powders. Their XRD patterns were the same as that (Figure 5(b)) of the powder obtained by calcination of *h*-$LaCO_3OH$. On the other hand, the polymorph of the $La_2O_2CO_3$ powders

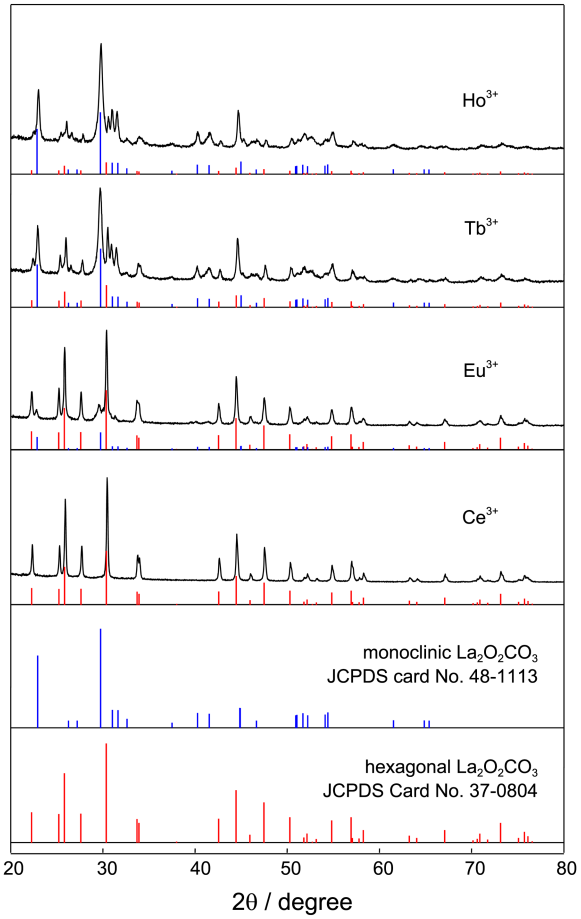


**Figure 6.** XRD patterns of samples obtained by calcination of *o*-$LaCO_3OH:Ln^{3+}$ (2 mol %, Ln = Ce, Eu, Tb, and Ho) at 600 °C for 2 h.

obtained by calcination of *o*-$LaCO_3OH:Ln^{3+}$ (2 mol %, Ln = Ce, Eu, Tb, and Ho) at 600 °C for 2 h depended on the dopants, as shown in Figure 6. Doping with 2 mol % $Ce^{3+}$ ion resulted in pure *h*-$La_2O_2CO_3$, but an increase in the doping concentrations of $Ce^{3+}$ ion caused the formation of monoclinic (*m*-) $La_2O_2CO_3$ (JCPDS Card No. 48-1113). Though not shown here, the calcination of *o*-$LaCO_3OH:Ce^{3+}$ (10 mol %) at 600 °C produced pure *m*-$La_2O_2CO_3$. The pure *m*-$La_2O_2CO_3$ was also obtained by calcination of $La(OH)_3$ at 400 °C for 2 h.[32] On the other hand, doping with $Eu^{3+}$, $Tb^{3+}$, and $Ho^{3+}$ ions resulted in a mixture of *h*- and *m*-$La_2O_2CO_3$. The relative quantity of the latter phase increased with decreasing ionic radius of the $Ln^{3+}$ ion.

The calcination of *o*-$LaCO_3OH:Ln^{3+}$ (2 mol %, Ln = Ce, Eu, Tb, and Ho) at 800 °C for 2 h yielded *h*-$La_2O_3$ powders, irrespective of the species of $Ln^{3+}$ ions. On the other hand, as shown in Figure 7, the calcination of *h*-$LaCO_3OH:Ln^{3+}$ (Ln = Eu and Tb) at 800 °C yielded an *h*-$La_2O_3$ powder with a very small amount of cubic $La_2O_3$ (ICCD–PDF # 98-005-1138 and 98-006-9895).

**Luminescence Properties of $LaCO_3OH:Eu^{3+}$ and $La_2O_2CO_3:Eu^{3+}$ Powders.** When acting as an emitting activator, the $Eu^{3+}$ ion is an excellent structural probe because of high sensitivity of its luminescence spectra to changes in local

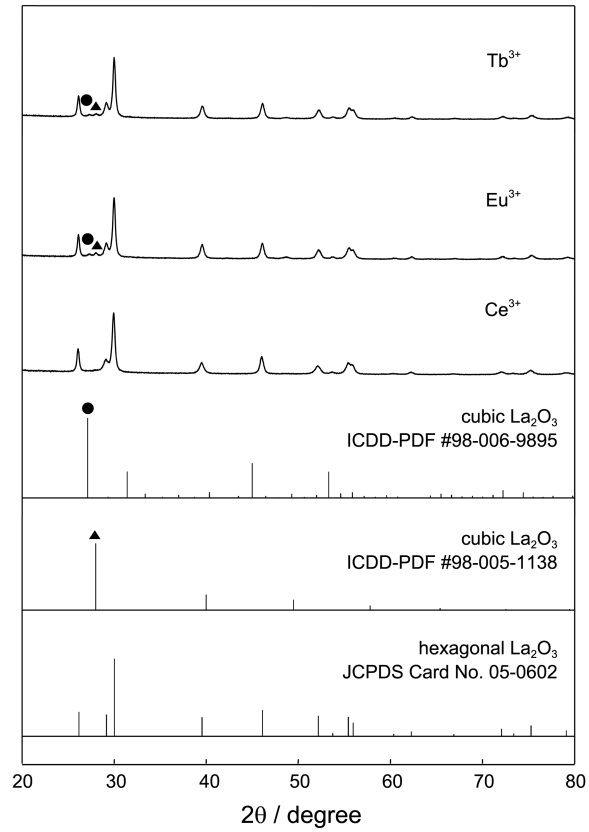


**Figure 7.** XRD patterns of samples obtained by calcination of *h*-$LaCO_3OH:Ln^{3+}$ (2 mol %, Ln = Ce, Eu, and Tb) at 800 °C for 2 h.

symmetry. The effect of the polymorph on the luminescence spectra was examined for $LaCO_3OH:Eu^{3+}$ (2 mol %) and $La_2O_2CO_3:Eu^{3+}$ (2 mol %) powders. As shown in Figures 8(a-1) and 8(a-2), the emission spectra (at $\lambda_{ex}$ = 395.8 nm) of

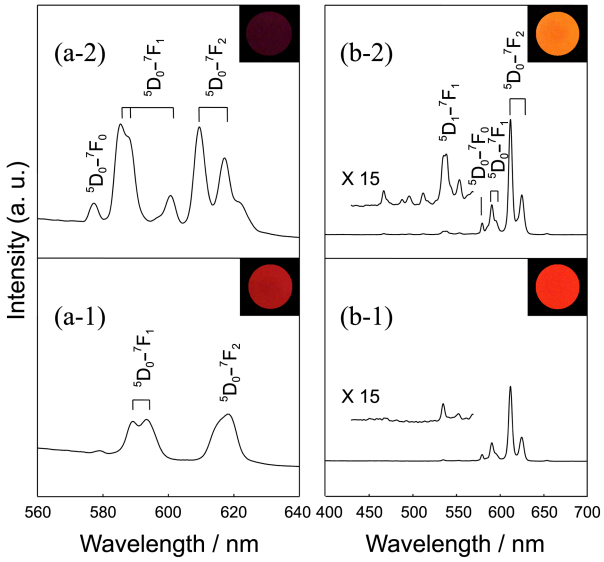


**Figure 8.** Emission spectra of (a-1) *h*- and (a-2) *o*-$LaCO_3OH:Eu^{3+}$ (2 mol %) powders ($\lambda_{ex}$ = 395.8 nm) and of samples obtained by calcination of (b-1) *h*- and (b-2) *o*-$LaCO_3OH:Eu^{3+}$ (2 mol %) powders ($\lambda_{ex}$ = 280.4 nm) at 600 °C for 2 h. The insets are their corresponding luminescence photographs at 254 nm UV lamp irradiation.

the *h*- and *o*-$LaCO_3OH$ powders were considerably different in shape, suggesting that the local symmetry of the $Eu^{3+}$ sites occupied in *h*- and *o*-$LaCO_3OH$ are different. The spectrum (Figure 8(a-1)) of *h*-$LaCO_3OH:Eu^{3+}$ showed two unresolved bands at *ca*. 590 and 618 nm, which were attributed to the $^5D_0 \rightarrow {}^7F_1$ and $^5D_0 \rightarrow {}^7F_2$ transitions, respectively. The appearance of the two unresolved bands indicated the presence of two $Eu^{3+}$ sites with similar local symmetry in *h*-$LaCO_3OH:Eu^{3+}$.

Figures 8(b-1) and (b-2) exhibit the emission spectra (at $\lambda_{ex} = 280.4$ nm) of $La_2O_2CO_3:Eu^{3+}$ (2 mol %) powders obtained by calcination of *h*- and *o*-$LaCO_3OH:Eu^{3+}$ (2 mol %) at 600 °C for 2 h. The emission bands were more intense for *o*-$LaCO_3OH:Eu^{3+}$ than for *h*-$LaCO_3OH:Eu^{3+}$, but both emission spectra had a similar shape. The similarity can be explained in terms of the polymorph, respectively. As discussed above, the sample derived from *h*-$LaCO_3OH:Eu^{3+}$ was a pure *h*-$La_2O_2CO_3$ powder, whereas the sample derived from *o*-$LaCO_3OH:Eu^{3+}$ was an *h*-$La_2O_2CO_3$ powder with a small amount of *m*-$La_2O_2CO_3$. As shown in the insets, the luminescence of four phosphors in Figures 8(a-1), 8(a-2), 8(b-1) and 8(b-2) were strong red, dark red, red, and vivid yellow-red to the naked eye, respectively, at 254 nm UV lamp irradiation.

## Conclusions

The polymorph of $LaCO_3OH$ prepared by a hydrothermal reaction depended on the reaction temperature, inorganic salt additive, species of $Ln^{3+}$ dopant, and solvent. The calcination of *o*-$LaCO_3OH:Ln^{3+}$ (2 mol %) powders at 600 °C yielded a mixture of *h*- and *m*-$La_2O_2CO_3:Ln^{3+}$ powders. The relative quantity of the latter increased with decreasing ionic radius of the $Ln^{3+}$ ion and increasing doping concentrations. On the other hand, the calcination of *h*-$LaCO_3OH:Ln^{3+}$ (2 mol %) powders at 600 °C gave a pure *h*-$La_2O_2CO_3:Ln^{3+}$ powder, irrespective of the species of $Ln^{3+}$ ion (Ln = Ce, Eu, and Tb). The emission spectra of the *h*- and *o*-$LaCO_3OH:Eu^{3+}$ were considerably different in shape, suggesting that the local symmetry of the $Eu^{3+}$ sites occupied in *h*- and *o*-$LaCO_3OH$ are different. The emission spectra of their thermal decomposition products at 600 °C had a similar shape due to the small difference in their polymorph.

**Acknowledgments.** This work was supported by the Energy Efficiency & Resources Program (No. 2011T100100081) and the Human Resources Development Program (No. 20124030200100) of the Korea Institute of Energy Technology Evaluation and Planning (KETEP) grant funded by the Korean government Ministry of Trade, Industry and Energy.

## References

1. Gaines, R. V.; Skinner, H. C. W.; Foord, E. E.; Mason, B.; Rosenzweig, A. *Dana's New Mineralogy*, 8th ed, John Wiley & Sons: New York, 1997; Class 15 and 16.
2. Shang, M.; Geng, D.; Kang, X.; Yang, D.; Zhang, Y.; Lin, J. *Inorg. Chem*. **2012**, *51*, 11106.
3. Li, G.; Peng, C.; Zhang, C.; Xu, Z.; Shang, M.; Yang, D.; Kang, X.; Wang, W.; Li, C.; Cheng, Z.; Lin, J. *Inorg. Chem*. **2010**, *49*, 10522.
4. Mao, G.; Zhang, H.; Li, H.; Jin, J.; Niu, S. *J. Electrochem. Soc*. **2012**, *159*, J48.
5. Li, G.; Shang, M.; Geng, D.; Yang, D.; Peng, C.; Cheng, Z.; Lin, J. *CrystEngComm* **2012**, *14*, 2100.
6. Loitongbam, R. S.; Singh, N. S.; Singh, W. R.; Ningthoujam, R. S. *J. Lumin*. **2013**, *134*, 14.
7. Wakita, H.; Kinoshita, S. *Bull. Chem. Soc. Jpn*. **1979**, *52*, 428.
8. Haschke, J. M. *J. Solid Chem*. **1975**, *12*, 115.
9. Sun, J.; Kyotani, T.; Tomita, A. *J. Solid Chem*. **1986**, *65*, 94.
10. Li, Z.; Zhang, J.; Du, J.; Gao, H.; Gao, Y.; Mu, T.; Han, B. *Mater. Lett*. **2005**, *59*, 963.
11. Pol, V. G.; Thiyagarajan, P.; Moreno, J. M. C.; Popa, M. *Inorg. Chem*. **2009**, *48*, 6417.
12. Han, Z.; Xu, P.; Ratinac, K. R.; Lu, G. Q. *J. Cryst. Growth* **2004**, *273*, 248.
13. Han, Z.; Yang, Q.; Lu, G. Q. *J. Solid Chem*. **2004**, *177*, 3709.
14. Zhang, Y.; Han, K.; Cheng, T.; Fang, Z. *Inorg. Chem*. **2007**, *46*, 4713.
15. Sun, C.; Xiao, G.; Li, H.; Chen, L. *J. Am. Ceram. Soc*. **2007**, *90*, 2576.
16. Xie, J.; Wu, Q.; Zhang, D.; Ding, Y. *Cryst. Growth Des*. **2009**, *9*, 3889.
17. Zhong, S.-L.; Zhang, L.-F.; Jiang, J.-W.; Lv, Y.-H.; Xu, R.; Xu, A.-W.; Wang, S.-P. *CrystEngComm* **2011**, *13*, 4151-4160.
18. Nguyen, T.-D.; Dinh, C.-T.; Do, T.-O. *Inorg. Chem*. **2011**, *50*, 1309.
19. Yang, X.; Zhai, Z.; Xu, L.; Li, M.; Zhang, Y.; Hou, W. *RSC Adv.* **2013**, *3*, 3907.
20. Ali, A. A.; Hasan, M. A.; Zaki, M. I. *Mater. Res. Bull*. **2008**, *43*, 16.
21. Akinc,M.; Sordelet, D. *Adv. Ceram. Mater*. **1989**, *2*, 232.
22. Woo, D. C.; Lee, M.-H.; Jung, W.-S. *Ceram. Int*. **2013**, *39*, 1533.
23. Mattijeviæ, E. *Pure Appl. Chem*. **1988**, *60*, 1479.
24. Qi, R.-J.; Zhu, Y.-J. *J. Phys. Chem. B* **2006**, *110*, 8302.
25. Ma, M.-G.; Zhu, Y.-J.; Chang, J. *J. Phys. Chem. B* **2006**, *110*, 14226.
26. Xia, T.; Li, Q.; Liu, X.; Meng, J.; Cao, X. Q. *J. Phys. Chem. B* **2006**, *110*, 2006.
27. Wang, M.; Huang, Q.-L.; Hong, J.-M.; Chen, X.-T.; Xue, Z.-L. *Cryst. Growth Des.* **2006**, *6*, 2169.
28. Kutty, T. R. N.; Tareen, J. A. K.; Mohammed, I. *J. Less-Common Met*. **1985**, *105*, 197.
29. Herzberg, G. *Infrared and Raman Spectra of Polyatomic Molecules*, D. Van Nostrand Co., New York, 1945; p 178.
30. Nakamoto, K. *Infrared and Raman Spectra of Inorganic and Coordination Compounds*, 3rd ed.; John Wiley & Sons: 1978; p 93.
31. Turcotte, R. P.; Sawyer, J. O.; Eyring, L. *Inorg. Chem*. **1969**, *8*, 238.
32. Mu, Q.; Wang, Y. *J. Alloys Compd*. **2011**, *509*, 396.